# Throughput Enhancement in Optical-Access-Enabled Cloud Radio Access Networks

Xinbo Wang, Lin Wang, Cicek Cavdar*, Biswanath Mukherjee
University of California, Davis
* KTH Royal Institute of Technology, Sweden
xbwang@ucdavis.edu

Massimo Tornatore+, Hwan-Seok Chung‡, Han-Hyub Lee‡, Soomyung Park‡
+ Politecnico di Milano, Italy
‡ ETRI, Korea

***Abstract*— Next-generation radio access networks (RAN) must enhance their throughput to meet the increasing traffic demands. We jointly consider virtual PON formation and coordinate multi-point transmission to achieve throughput enhancement in optical-access-enabled Cloud RAN (CRAN).**

***Keywords—5G; CRAN; Throughput; Optical network***

## I. Introduction

Cisco's visual network index [1] reports that the IP data handled by access networks has been increasing massively, from under 3 exabytes in 2010 to 190 exabytes expected by 2018, on pace to exceed 500 exabytes by 2020. Such fast-increasing traffic demand is urging network operators to significantly enhance the throughput of their access network.

Optical networks can provide the infrastructure (often referred as 5G transport) to enhance the throughput of radio access network (RAN) by enabling advanced radio techniques, e.g., Coordinated Multi-Point (CoMP) transmission/ reception. CoMP is a suite of radio-coordination techniques to reduce inter-cell interference (ICI) and increase system throughput. Among CoMP techniques providing highest gains, Joint Transmission (JT) is the one we shall study. JT is applied in contexts where multiple adjacent cellular base stations (BSs) cooperate to transmit and receive signals for a user equipment (UE) over the same physical resource block (the spectrum band of a RU is divided into continuous physical resource block with fixed size, which can be referred as "resource block" or "RB" for short) so that ICI can be converted to useful information. But traditional distributed RAN (DRAN) cannot effectively support JT as data and scheduling information has to be exchanged fast and available at all BSs before JT decision is taken [2]. Recently, a cloud-RAN architecture has been proposed [3], which can support the JT technique. CRAN decomposes the traditional BS into a "digital unit" (DU), responsible for baseband processing, and a "radio unit" (RU), responsible for digitizing and receiving/transmitting radio signals. RUs are at cell sites, while DUs are centralized in one location, called DU cloud, which can ease the implementation of JT. DUs provide centralized baseband processing for multiple coordinating BSs (JT set) for a UE . However, the digitized (but not baseband-processed) data exchanged between DU cloud and RUs requires a high-capacity network, which is referred to as "fronthaul", as opposed to backhaul in DRAN. To achieve a high-performance JT, integrated control and management of RAN along with the distribution network is also needed, which is the focus of our study.

TWDM-PON is a promising fronthaul solution for CRAN [4] due to its abundant bandwidth, low latency, and low cost. Also, a TWDM-PON can dynamically configure the association of optical network units (ONUs) to the optical line terminal (OLT) transceiver, i.e., linecard (LC), by retuning their serving wavelength. Over the same wavelength, many ONUs can communicate as in an independent PON, called virtual PON (VPON). Multiple VPONs can be provided by a TWDM-PON over different wavelengths; and such VPONs can be dynamically formed for different purposes--energy saving, handover reduction, hot-spot coverage, and load-balancing--by following/adapting to the traffic pattern in the RAN [5]. As in the example shown in Fig. 1, we can form a (round) VPON for an ongoing event in a stadium, a (square) VPON for a shopping center during holiday time, or a (linear) VPON along a railway track.

Our study investigates the problem of maximizing the number of UEs supported by JT services by effectively forming VPONs that can associate multiple BSs to the same JT controller. RBs must also be properly assigned to UEs so that ICI is minimized. We first describe the considered TWDM-PON-based architecture for CRAN. Then, we present a mathematical model to maximize the overall throughput and show that CRAN with VPON formation (VF) can achieve significant throughput enhancement compared to CRAN without VF and DRAN.

## II. An Optical-Access- enabled Transport Architecture for CRAN

Fig. 2 shows the TWDM-PON based optical access architecture for CRAN considered in this study. In the upstream, every cell equips the RU with an ONU that can transport the digitized signals from RU to OLT. The WDM multiplexer separates each wavelength to its serving LC, which sends the signal received over the wavelength to the connected DU. Each DU is implemented on a general-purpose server equipped with dedicated hardware/software as a JT controller (considering that a single JT controller for the whole CRAN is not scalable). By reconfiguring the wavelengths, the VPON can dynamically associate multiple RUs with a single DU, whose computing power and cached data can be shared. For example, in Fig. 2, $DU_2$ is shared by $RU_2$ and $RU_3$ by configuring their serving wavelength to $\lambda_2$.

This work was supported by Institute for Information & communications Technology Promotion (IITP) grant funded by the Korea government (MSIP) (B0132-15-1004, SDN based wired and wireless converged optical access networking).

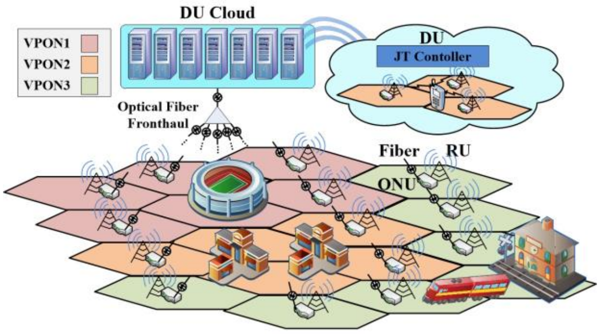


Fig. 1. Illustration of CoMP and VPON Formation

Note that the flexibility of VF can ease the implementation of JT as follows. To achieve high performance, JT requires heavy computation and short latency [2]. But the computing power of traditional BS is not designed for JT and thus insufficient to achieve high performance JT in traditional settings. Also, data and scheduling information should be duplicated and distributed to all coordinating BSs before the scheduling decision is taken (≤ 4 ms) [2]. But the signaling exchange in the distributed architecture of DRAN may undergo long delay (10-20 ms) over the backhaul links, which can degrade the performance of JT. Such delay can be shortened in the architecture considered here for two reasons. First, TWDM-PON can provide many VPONs (wavelengths) with high bandwidth to concurrently transport and process the digitized signals. Second, the JT controller in a DU can take scheduling decisions as soon as it gets fronthaul data containing the scheduling information and quickly broadcast them to the coordinating BSs over the same VPON.

## III. Throughput-Enhancement Maximization Problem

We propose the throughput enhancement maximization problem to provide more UEs with JT service through VF (wavelength assignment), while assigning RBs to UEs so that ICI is minimized. Although VF can assist JT in providing stronger signal (and thus higher throughput) for the supporting UEs because of the joint transmission of signals over same RB from multiple BSs, the stronger signal can cause ICI for other UEs if they are assigned the same RB in neighboring BSs, and thus their throughput will be degraded. This situation can be avoided by assigning different RBs to UEs, but when traffic load increases, it is hard to assign RBs without conflict due to the diminishing available RBs. Excessive JT services will consume RBs more rapidly, aggravate ICI, and thus degrade the overall throughput. But proper VF and RB assignment can trade-off between providing JT services and reducing ICI in order to maximize the overall throughput in Eqn. (1).

We present a constraint programming (CP) model to solve this problem.

### A. Given

- I: set of UEs.
- C: set of cells.
- W: number of wavelengths.
- R: number of RBs per cell.

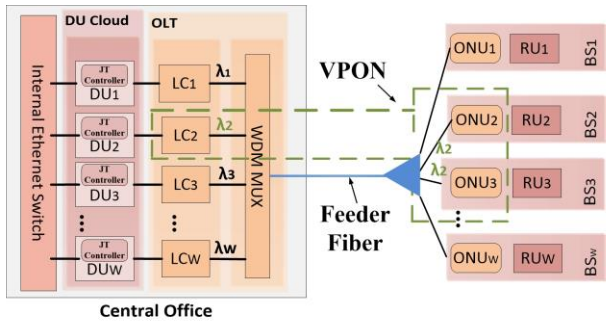


Fig. 2. Architecture of TWDM-PON-based CRAN.

- Cap: the bandwidth capacity of a wavelength.
- $C_i$=$c_i \cap \{c_i'\}$: the set of cells that a UE $i$ can receive signal from, where $c_i$ is the host cell where UE $i$ locates, and $\{c_i'\}$ are other cells.
- $I_c$: the set of UEs that cell c can send signal to.

### B. Integer Variables

- $f_{i,c} \in \{0..\mathrm{R}\}, \forall i \in I, \forall c \in C_i$: 0, UE i does not occupy any RB at cell c. Otherwise, the index of RB that UE $i$ occupies at cell c.
- $s_{i,c} \in \{0..1\}, \forall i \in I, \forall c \in C_i$: 1, if cell c is selected into the JT set of UE i. 0, otherwise.
- $t_{i,c} \in \{0..1\}, \forall i \in I, \forall c \in C_i$: 1, if UE i receives ICI from cell c. 0, otherwise.
- $w_c \in \{1..|W|\}, \forall c \in C$: the wavelength assigned to cell c.
- $m_{c,f} \in \{0..1\}, \forall c \in C, \forall f \in \{1..F\}$ : whether RB f is occupied at cell c.
- $n_c \in \{0..\mathrm{F}\}, \forall c \in C$: the number of RBs occupied at cell c.

We consider two ways to reduce the complexity of variables for the model. First, we only create a variable that will be used in the model. For example, for each UE i, we only create variable $f_{i,c}$ for cells that the UE can receive signals from, $C_i$. Second, instead of creating a three-dimension binary variable $f_{i,c,r}$ to indicate whether RB r of cell c is assigned to UE i, we use a two-dimension variable $f_{i,c}$ with domain {1..R}, which restricts the value that can be assigned to the variable within the bandwidth resources of a RU. This reduce the complexity from $2^{|I|\cdot|C|\cdot R}$ of $f_{i,c,r}$ to $R^{|I|\cdot|C|}$ for any R, for proof see Appendix I. The same technique is used also for variable $w_c$.

### C. Objective

The objective is to maximize the total throughput of all UEs in the network. To calculate the data rate for each UE, we use the Shannon capacity formula.

$$\sum_{i\in I} B\log_2\left(1+\frac{\sum_{c\in C_i} s_{i,c} P G_{i,c}}{\sum_{c'\in\{c_i'\}} t_{i,c'} P G_{i,c'} + BN_0}\right) \tag{1}$$

where $B$ is the fixed bandwidth of one RB. $P$ is the fixed transmission power assigned to one RB at a RU. $G_{i,c}$ is the pre-calculated channel gain between UE i and cell c. RBs in the spectral band of a cell are assigned to UEs equally where each UE gets maximum one RB.

### D. Constraints

$$f_{i,c_i} > 0 \qquad \forall i \in I \quad (2)$$

This constraint ensures that the RU at the host cell $c_i$ of UE i must be in the UE's JT set and assign it a RB. Other cells, $\{c_i'\}$, that can send signals to UE i might not be chosen into its JT set, so their variables $f_{i,c}(\forall c \in \{c_i'\})$ can have value 0.

$$s_{i,c} == (f_{i,c} > 0) \quad \forall i \in I, \forall c \in C_i \quad (3)$$

This constraint ensures that Cell c is in JT set of UE i if and only if UE i occupies a RB at Cell c. In constraint programming, a relational constraint, e.g. $f_{i,c} > 0$, can used in a value context, where it evaluates to 0 or 1.

$$m_{c,f} == count(\{f_{i,c}\}_{i \in I_c}, f) \quad \forall c \in C, \forall f \in \{1..F\} \quad (4)$$

This constraint ensures that a RB f is occupied at Cell c if and only if it is assigned to a UE. In constraint programming, the *count* constraint can count the number of variables in an array, $\{f_{i,c}\}_{i \in I_c}$, that are assigned value f. Since the count must be equal to the value of variable $m_{c,f}$, whose is at most 1. So this constraint also requires that a RB f cannot be assigned to more than 1 UE at a time.

$$s_{i,c} == (f_{i,c} == f_{i,c_i}) \quad \forall i \in I, \forall c \in C_i \quad (5)$$

This constraint ensures that Cell c is in the JT set of UE i if and only if the cell provides UE with the same RB as the one assigned by the host cell of UE. In other word, all cells in the JT set of a UE must transmit signals over the identical RB to the UE, which we call **resource-block-continuity constraint**.

$$s_{i,c} => (w_c == w_{c_i}) \qquad \forall i \in I, \forall c \in C_i \quad (6)$$

This constraint ensures that if Cell c is in the JT set of UE i then Cell c must tune its ONU onto the same wavelength of the host cell of UE i. In other word, all cells in the JT set of at UE must tune their ONU onto the same wavelength so that they can be associated with the same DU, which we call **wavelength-uniformity constraint**. In constraint programming, the *infer* constraint, a => b, can specify that if constraint a is true, then constraint b must be true.

$$t_{i,c} == (s_{i,c} == 0)\, AND\, (m_{c,f_{i,c_i}} > 0) \quad \forall i \in I, \forall c \in C_i \quad (7)$$

This constraint ensures that UE i is interfered by Cell c if and only if (1) Cell c is not in its JT set, and (2) Cell c provides other UE with the same RB that is assigned to UE i by its host cell, which means RBs assigned by Cell c and the host cell of UE i are overlapping. In constraint programming, the latter can be modeled using the element constraint:

$$m_{c,f_{i,c_i}} = element(M, y) > 0$$

which states that the y-th variable in an array of variables, $M = \{m_1, m_2, \ldots m_k\}$ must be larger than 0. Here, M is $\{m_{c,f}\}_{f \in \{1..F\}} = \{m_{c,1}, m_{c,2}, \ldots, m_{c,F}\}$, and y is the variable $f_{i,c_i}$, which specifies the index of RB occupied by UE i at its host cell $c_i$.

$$n_c == \sum_{i \in I_c} (f_{i,c} > 0) \qquad \forall c \in C \quad (8)$$

This constraint the number of occupied RBs at Cell c must be equal to the number of UEs that are assigned RBs from it.

$$\sum_{c \in C} (w_c == \lambda) \cdot \mathrm{H}(n_c) \le Cap \quad \forall \lambda \in \{1..W\} \quad (9)$$

This constraint ensures that the total CPRI data rate of cells that are using the a given wavelength λ must be no larger than the capacity of a wavelength, Cap. $H(\cdot)$ is a calculator that takes number of occupied RBs at a cell as input and generates the CPRI data rate needed by the cell. According to [6], given the number of antennas, resolution of the symbol representation and CPRI overhead, H solely depends on the sampling rate. So it is not the CPRI protocol that determines the CPRI rate, but the sampling rate of the RU. There are various ongoing works that tries to compress CPRI rate and make it dependent on the load of a cell [7] [8]. One idea is to remove the redundancy in spectral domain caused by oversampling on unused RBs, so that the sampling rate (and thus $H(\cdot)$) is a linear function of the number of occupied RBs at a cell.

## IV. Illustrative Numerical Results

In this section, we quantitatively demonstrate how V-CRAN can outperform the two reference architectures--DRAN and CRAN--with respect to throughput, and where the enhancement comes from. In DRAN, every DU is collocated with its RU at the cell site. Hence, a cell needs independent "housing" facility, DU remains active all the time, and no inter-cell coordination is deployed at the cell. In traditional CRAN, although DUs are co-located in the DU hotel, there is no sharing of DUs and wavelength, thus every cell needs an active DU and optical transceiver dedicated to service it, and only limited inter-cell coordination is deployed (ICIC but no JT). We assume simple CRAN architecture as an intermediate state of RAN evolution because it help us understand where the superiority of V-CRAN comes from and by how much.

TABLE I. SIMULATION PARAMETERS

| Parameters | Value |
|---|---|
| Deployment | 19 BS, ISD=500M, hexagonal grid, wrap-around |
| Path loss | L=15.3+37.6log(d) (3GPP Typical Urban) |
| Shadow fading | std dev 8 dB |
| Spectral Bandwidth | 5~20 MHz (group into 5 RBGs) |
| Wavelength Bandwidth | 10 Gbps |
| Max RU $P_{TX}$ | 20 W (4 W/RBG) |
| UE sensitivity | -90 dBm |
| Noise PSD | -174 dBm/Hz |
| Power consumption | $P_s$=50 W, $P_{H,D}$=600 W, $P_{H,Pool}$=500 W, $P_{DU}$=100 W/DU, $P_{LC}$=5 W/LC, $P_{ONU}$=7.7 W/ONU |

Simulation parameters are reported in Table I [9]. For the sake of simplicity omnidirectional antennas have been considered instead of sectored sites. RBs of a cell can be grouped into 5 larger resource block groups (RBGs), and assigned to UEs equally where each user gets maximum one RBG. The number of UEs that are stationary and uniformly distributed in the network has been set from 9 to 90, according to the utilization factor (u-factor)m which is the ratio of the number of UEs (equal to the number of occupied RBGs in DRAN scenario) to the total number of RBGs in the network.

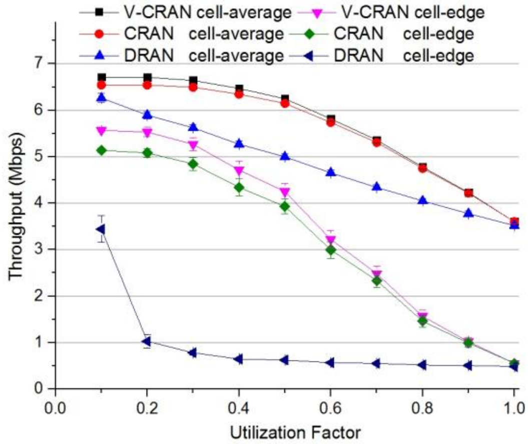


Fig. 3 Comparing the average throughput (per user) for all users (cell-average) and 5% worst case users (cell-edge) with 10 MHz bandwidth.

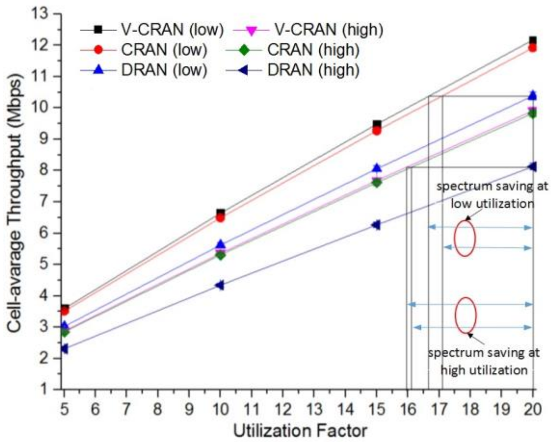


Fig. 4 Comparing the cell-average throughput at low u-factor (0.3) and high u-factor (0.7), respectively.

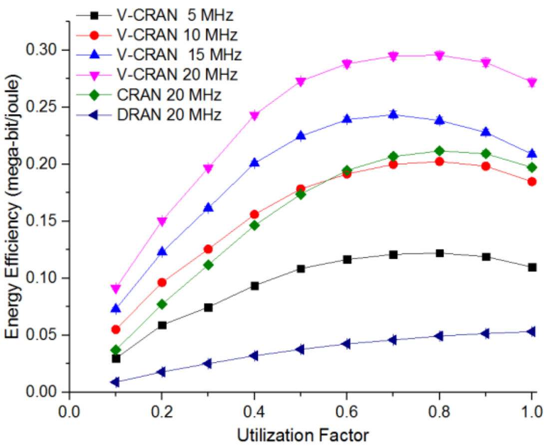


Fig. 5 Energy efficiency (mega-bit/joule) vs. load ratio with 10 MHz spectral bandwidth.

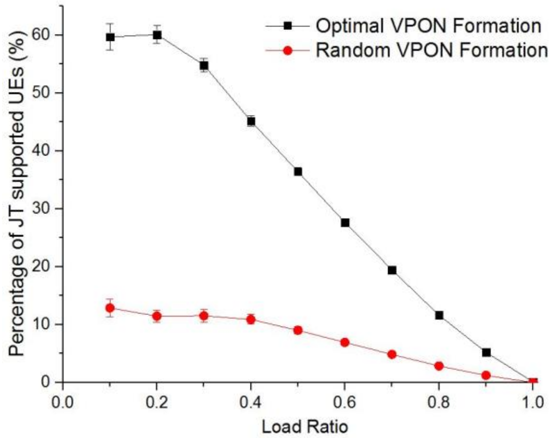


Fig. 6 Percentage of UEs supported by JT service vs. load ratio for optimal VPON formation and random VPON formation with 10 MHz spectral bandwidth.

Fig. 6 En

For example, u-factor equal to 1 gives the maximum load of the network, where each UE gets one RBG from its host cell and all RBGs in a cell have been occupied. We use IBM CP Optimizer to solve the constraint programming model with optimal results, which is proven by demonstrating that there is no better solution in the search space than the current optimal solution. Each result at a given u-factor is obtained by statistical analysis considering 200 simulations runs and a 95% confidence interval.

In Fig. 3, we plot the average throughputs for cell-average and cell-edge users, respectively, as the changing of utilization factor ("u-factor"). Each cell has 10 MHz bandwidth. DRAN achieves the lowest throughput and suffers sharp throughput degradation because there is more interference when u-factor becomes larger. CRAN also achieves better performance than DRAN (at most 23% and 573% for cell-average and cell-edge users, respectively), because ICIC can reduce the interference, especially for low u-factor, where it is easier to avoid overlapping between RB-user assignments when RB resources are more sufficient. V-CRAN can further enhance the throughput because of JT, with about 25% improvement for cell-average users compared to DRAN, and the throughput enhancement is more significant for cell-edge users (almost 645%). But when u-factor becomes larger, there is less throughput enhancement for V-CRAN, because a VPON can accommodate fewer cells, and thus less JT services can be provided.

In Fig. 4, we plot the cell-average throughput of the three architectures for available bandwidth of each cell ranging from 5 to 20 MHz under two scenarios: low and high u-factors. Confirming Fig. 3a, V-CRAN achieves the highest throughput for various spectral bandwidth availability. We note the bandwidth saved by V-CRAN and CRAN to achieve the same throughput of DRAN with 20 MHz configuration. For high u-factor, V-CRAN and CRAN save around 4.05 MHz (20.3%) and 3.85 MHz (19.3%), respectively. For low u-factor, V-CRAN and CRAN save around 3.4 MHz (17%) and 2.9 MHz (14.5%), respectively. The superiority of V-CRAN is more noticeable when u-factor is small, confirming Fig. 3. Results in Fig. 4 shows that the evolution of network architecture can not only bring higher data-transmission rate, but also more efficient use of precious spectral bandwidth.

In Fig. 5, we further compare the energy efficiency of V-CRAN with bandwidth from 5 MHz to 20 MHz with CRAN and DRAN with 20 MHz bandwidth. Note that energy efficiency is the number of bits that can sent by consuming one joule. For 20 MHz bandwidth, V-CRAN achieves much higher energy efficiency than CRAN and DRAN because it can enhance the throughput as well as reduce the power consumption. For the detailed study about power saving of V-

CRAN, please refer to our work in [10]. The energy efficiency of V-CRAN is higher when each cell has more bandwidth, because much more throughput can be achieved by consuming a bit more power incurred by DUs and wavelengths. We also plot the energy efficiency of CRAN and DRAN with 20 MHz bandwidth. To achieve the same energy efficiency of CRAN, V-CRAN only needs half bandwidth, 10 MHz. And V-CRAN with only 5 MHz is much more energy-efficient than DRAN with 20 MHz. We also find that optimal energy efficiency can be achieved when u-factor is around 0.7~0.8.

In Fig. 6, we plot the percentage of UEs that are supported by JT service with optimal VPON formation and random VPON formation. In general, the percentage of JT-supported UEs decreases with the increase of u-factor. Because when u-factor increases, a VPON can accommodate fewer cells so wavelength-uniformity constraint is harder to satisfy, and more RBs are occupied so resource-block-continuity constraint is harder to satisfy. For a given u-factor, random VPON formation provides much less UEs with JT service because it does not consider the inter-cell coordination when associating cells to a DU.

## V. Conclusion

5G mobile networks need to provide higher data rates with the advanced radio transmission techniques, e.g. Coordinated Multi-Point (CoMP) transmission/reception. Cloud radio access network (CRAN) centralizes digital unit (DU) of base station (BS) to a central office, but how it can support CoMP has not reached a consensus yet. In this article, we present an virtualized CRAN (V-CRAN) that use a high-speed optical transport network, viz. time-wavelength division multiplexing passive optical network (TWDM-PON) to transport the traffic between digital units and radio units. We leverage the concept of "virtualized-BS" that can be optimally formed to enhance the throughput of a UE by exploiting virtualized resources. We formulate a throughput enhancement optimization model using constraint programming. Simulation experiments show that V-CRAN can achieve much higher throughput and is more energy-efficient compared with CRAN and traditional distributed RAN.

## References

[1] Cisco, "Visual Networking Index: Forecast and Methodology, 2014–2019", May. 2015.

[2] Next generation mobile network alliance, "RAN Evolution project CoMP evaluation and enhancement," Mar. 2015.

[3] China Mobile Research Institute, "C-RAN: The road towards green RAN V3.0," Dec. 2013.

[4] D. Iida *et al.*, "Dynamic TWDM-PON for Mobile Radio Access Networks," *Optics Express,* vol. 21, no. 22, pp. 26209-26218, 2013.

[5] R. Wang et al., "Energy Saving via Dynamic Wavelength Sharing in TWDM-PON," *IEEE JSAC,* vol. 32, no. 8, pp. 1566-1574, Aug. 2014.

[6] Next generation mobile network alliance, "Further Study on Critical C-RAN Technologies," Mar. 2015.

[7] B. Guo et al., "LTE/LTE-A Signal Compression on the CPRI Interface," *Bell Labs Tech. Journal*, vol. 18, no. 2, pp. 117-133, Sept. 2013.

[8] T.X. Vu et al., "Adaptive Compression and Joint Detection for Fronthaul Uplinks in Cloud Radio Access Networks," *IEEE Transactions on Communications*, vol. *63*, no. 11, pp. 4565-4575, Nov. 2015.

[9] "Further advancements for E-UTRA physical layer aspects v.9.0.0," 3GPP TR 36.814, 2010.

[10] X. Wang et al., "Energy-Efficient Virtual Base Station Formation in Optical-Access-Enabled Cloud-RAN," *IEEE J. on Selected Areas in Commun.*, vol. 34, no. 6, Jan. 2016.